engineering proceedings

Proceeding Paper

Computational Investigation of the Flow Structure through an Over-Expanded Nozzle †

Muhammad Haroon [1,*], Shummaila Rasheed [1], Muhammad Irfan [1], Manzar Masud [1] and Muhammad Arsalan Munawar [2]

1 Department of Mechanical Engineering, Capital University of Science and Technology (CUST), Islamabad 44000, Pakistan
2 Department of Mechanical Engineering, International Islamic University, Islamabad 44000, Pakistan
* Correspondence: muhammad.haroon@cust.edu.pk

† Presented at the 2nd International Conference on Advances in Mechanical Engineering (ICAME-22), Islamabad, Pakistan, 25 August 2022.

Abstract: Flow separation is a complex phenomenon that occurs in many internal and external flows. In internal flows, flow separation produces so-called side loads that are undesirable. This study aims to investigate the effect of the nozzle-pressure ratio on flow structures in a non-axisymmetric sub-scale two-dimensional (2D) convergent divergent type and in a three-dimensional axisymmetric nozzle, computationally. State-of-the-art ANSYS CFX software is used for the numerical flow analysis at two different pressure ratios: 3.0 and 3.4. Computational analysis shows that the flow is dominated by induced shock-wave boundary-layer separation. The computational results are in good agreement with the available experimental data. A considerable difference between the flow structure is observed from 3.0 to 3.4 NPRs.

Keywords: flow separation; over expanded; side loads; supersonic nozzle

Citation: Haroon, M.; Rasheed, S.; Irfan, M.; Masud, M.; Munawar, M.A. Computational Investigation of the Flow Structure through an Over-Expanded Nozzle. *Eng. Proc.* **2022**, *23*, 7. https://doi.org/10.3390/engproc2022023007

Academic Editors: Mahabat Khan and M. Javed Hyder

Published: 20 September 2022

1. Introduction

Nozzle-flow separation is a natural gas dynamics phenomenon that occurs in supersonic convergent divergent nozzles when they operate below its design nozzle pressure ratio (NPR), also called operation in over-expanded conditions. Over expanded operating conditions may occur during startup and throttling processes. It seems in the first instance that there is an overexpansion of the nozzle's enhanced thrust efficiency and control mass flow rate, but the resultant flow separation creates some serious issues for the designing of over-expanded nozzles [1]. Fluid adjusts itself inside the nozzle to fulfil the exit boundary conditions (pressure) and forms Mack disks; incident shocks; shock-wave interactions; shock-wave boundary layer interactions (SWBLIs), and also changes the entire internal geometry of the nozzle [2]. SWBLIs are the most undesirable phenomenon in nozzle designs. SWBLIs create side loads that not only damage the nozzle, but also place life-limiting constraints on the nozzle design [3].

Flow separation and its related phenomena are of great interest to researchers. Based on these phenomena, various analytical, computational, and experimental studies on sub-scale and full-scale models have been conducted [4]. Early studies reported that flow separation from the wall occurs due to the fluid's viscous effect and high pressure gradient across the flow when the nozzle operates at a low nozzle-pressure ratio (NPR) and with a comparatively large expansion ratio [1]. Later on, it was determined that there are two types of flow regimes existing in flow separation: one is called FSS (free shock separation), in which flow is completely detached from the nozzle and never reattached to the wall boundary. The second is called RSS (restricted shock separation) shown by a recirculatory bubbles on the nozzle wall where flow is first detached downstream of the nozzle and then reattached to the wall. In 1970, during the SSME (space shuttle main engine) experiment, the largest side-load was produced in the transition of FSS to RSS, while both flow regimes occurred at different nozzle-pressure ratios [3].

In the present study, the investigation of the flow structure using the geometric profile of an experimental sub-scale test CD-type nozzle is performed by considering two computation scenarios, namely, a 2D and 3D axisymmetric simulations. The main objective is to computationally analyze the flow structure of an over-expanded nozzle at higher pressure ratios.

2. Methodology

2.1. Geometry and Meshing

The experimental test nozzle employed in the current analysis was a non-axisymmetric; subscale; two-dimensional CD-type nozzle having a nominal throat area (At = 4.317 in2); expansion ratio (Ae/At = 1.797); and a constant width of 3.99 in. By keeping in mind the one-dimensional theory, the nozzle was designed with NPR = 8.78 and exit Mach number (Me) = 2.07, as presented in Figure 1a. By using the same profile of the geometry, computation was performed on the axisymmetric three- and two-dimensional nozzles. The geometry, mesh with quadrilateral elements, and domain of a 1D axisymmetric convergent–divergent nozzle are presented in Figure 1b. Moreover; Figure 2a shows the 3D axisymmetric geometry and Figure 2b shows the 3D axisymmetric mesh.

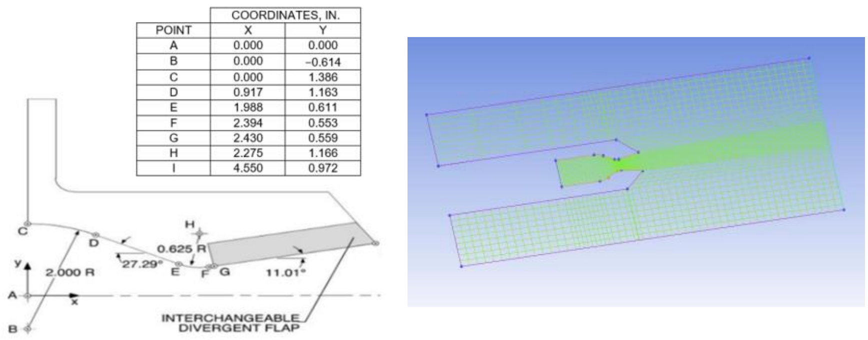

(**a**) (**b**)

Figure 1. (**a**) Geometry of 1D axisymmetric nozzle and (**b**) 2D geometry, mesh, and domain of an axisymmetric convergent–divergent nozzle.

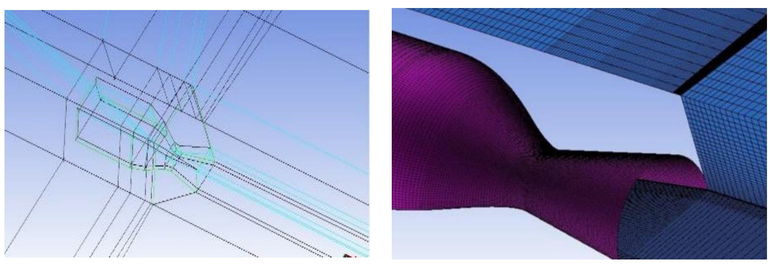

(**a**) (**b**)

Figure 2. (**a**) Three-dimensional axisymmetric geometry and (**b**) 3D axisymmetric mesh.

2.2. Computational Methods

Primarily, governing equations (Equations (1)–(4)) were transformed from the physical to computational domain by generalizing the method of co-ordinate transformation to increase the correctness of the numerical technique and implementation of boundary conditions. Later, the control volume technique was used to discretize these equations. The 2nd-order upwind scheme was employed to discretized the convective terms in the equations, whereas 2nd-order flux splitting was employed to drive inviscid fluxes to achieve the required up-winding and dissipation in the vicinity of the shock waves. The interface flux, which depends upon the upstream and downstream of the face, was determined by the separate terms. Diffusion terms were discretized using central differencing. The least-square cells technique was implemented to rebuild the variable gradients. A TVD slope limiter with the integration of the Minmod function was used, which limited the overshoots/undershoots on the cell faces. To control the numerical stiffness running at a low Mach number, a block Gauss-Seidel algorithm was solved in a coupled way to discretize the whole system. For the time derivatives, an advanced form of the 2nd-order Euler backward scheme, which is an implicit multistage time-stepping scheme, was used to obtain the physical time. On the other hand, for inner iteration, an implicit pseudo-time marching scheme was used.

$$\partial\rho/\partial t + \partial(\rho u_i)/\partial x_i = 0;\ \text{(Equation of Continuity)} \tag{1}$$

$$\partial(\rho u_i)/\partial t + \partial(\rho u_i u_j)/\partial x_j = -\partial p/x_i + \partial\tau_{ij}/\partial x_j;\ \text{(Momentum Equation)} \tag{2}$$

$$\partial\,(\rho E)/\partial t + \partial\,(u_i(\rho E + p)/\partial x_i = \vec{\nabla}.\,(\alpha_{eff}\partial T/\partial x_i + u_j(\tau_{ij});\ \text{(Energy Equation)} \tag{3}$$

$$\rho = p/RT;\ \text{(Gas Law)} \tag{4}$$

In Equations (1)–(4), E represents the total energy $((h-p)/\rho + (u^2+v^2)/2))$; ρ is the density (kg/m^3); u is the x-component of the velocity; t is the time (s); x is the location in the x direction; τ is the viscous stress tensor; p is the static pressure (kPa); R is the universal gas constant (J/kg K); and T is the temperature in kelvin.

2.3. Domain and Boundary Conditions

In this research, numerical analysis was performed on 3D and 2D symmetric conditions. Nozzle topology with the grid is presented in Figures 1 and 2. Downstream and upper boundaries were located at the heights of 40 and 100 in from the nozzle-throat section. The size of the domain was free of flow reflection from the boundaries. The NPR (ratio of total inlet pressure to the back pressure) was oscillated sinusoidally, whereas the back pressure was maintained at 1.3 kPa.

2.4. Initial and Boundary Conditions

At the boundary entrance of the nozzle, the stagnation temperature and pressure were considered as the physical boundary conditions and the remaining parameters were extracted by applying numerical boundary conditions using the Riemann invariant. Furthermore, the x and k values were specified as 61,979.31/s and 1.22 m^2/s^2 at the inlet domain, respectively. The outlet boundary conditions were restricted with exit-pressure boundary conditions. The adiabatic wall and non-slip boundary conditions were employed at the solid boundaries. The wall pressure achieved from a zero-pressure gradient acted normally on the nozzle-body surfaces. The inlet temperature of the nozzle was adjusted at 298.15 K.

3. Results and Discussions

Experimental normalized centerline static pressures (p/p_0) vs. nondimensionalized stream-wise locus relative to the throat of the nozzle are presented in Figure 3a,b. The results are the representations of a classical, experimental CD-type nozzle flow and three-dimensional axisymmetric CD-type nozzle. For NPRs of 3.4 and 3.0, pressure data points indicate an internally choked, over-expanded flow producing a frail shock near the nozzle throat. The shock downstream flow started to recover at an ambient pressure (p/p_0 = 1/NPR) in a continuous pulsating fashion in an experimental nozzle. The focused schlieren flow visualization of the experimental results obtained at NPR = 3.4 are presented in Figure 4a,b. This represents a frail, oblique, downstream shock at the nozzle throat having a lambda footprint structure. However, this study at NPRs of 3.0 and 3.4 presented an oblique shock near the throat and expanding downstream. The pressure adjusted itself to an ambient pressure in a pulsating manner. The difference between the present and experimental works is clear from comparing the shock locations and boundary-layer separation points. Due to a large surface area compared to the actual experimental nozzle, the near-wall viscous effects of the flow were the dominant cause of the shock-wave boundary-layer separation and its interactions with shocks.

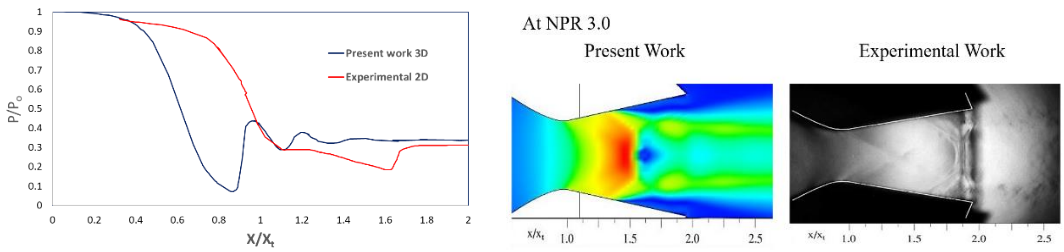

(**a**) (**b**)

Figure 3. (**a**) Graphical and (**b**) visual comparisons between the present study and the schlieren images of the experimental study at NPR = 3.

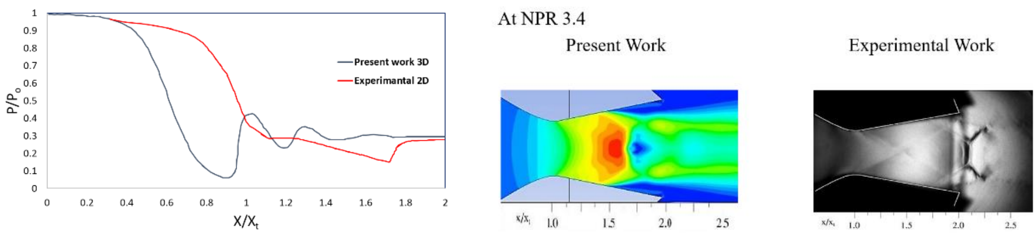

(**a**) (**b**)

Figure 4. (**a**) Graphical and (**b**) visual comparisons between the present study and the schlieren images of the experimental study at NPR = 3.4.

4. Conclusions

A computational study on an axisymmetric convergent–divergent nozzle was conducted in this research. A shock-induced boundary-layer-separation phenomenon occurred due to the dominant viscous effects observed in an axisymmetric three-dimensional nozzle in the design of over-expanded conditions during supersonic flow. A fully detached flow can clearly be seen in Figures 3 and 4 at NPRs of 3.0 and 3.4, respectively. In the axisymmetric three-dimensional CD-type nozzle, a flow-separation point occurred in half of the divergent portion as compared to the non-axisymmetric two-dimensional CD-type nozzle, because of its tendency for flow separation at supersonic speed due to viscous effects.

Author Contributions: Conceptualization; M.H. and S.R.; methodology; S.R.; software; S.R.; validation; S.R., M.I. and M.M.; formal analysis; S.R.; investigation; M.I.; data curation; M.M. and M.A.M.; writing—original draft preparation; S.R.; writing—review and editing; M.H. and M.A.M.; supervision; M.I. All authors have read and agreed to the published version of the manuscript.

Funding: This research received no external funding.

Institutional Review Board Statement: Not applicable.

Informed Consent Statement: Not applicable.

Data Availability Statement: Not applicable.

Conflicts of Interest: The authors declare no conflict of interest.

References

1. Lawrence, R.A. *Symmetrical and Unsymmetrical Flow Separation in Supersonic Nozzles*; NASA: Washington, DC, USA, 1967.
2. Hunter, C.A. Experimental Investigation of Separated Nozzle Flows. *J. Propuls. Power* **2004**, *20*, 527–532. [CrossRef]
3. Nave, L.; Coffey, G. Sea Level Side Loads in High-Area-Ratio Rocket Engines. In Proceedings of the AIAA/SAE 9th Propulsion Conference, Las Vegas, NV, USA, 5 November 1973.
4. Chen, C.L.; Chakravarthy, S.R.; Hung, C.M. Numerical Investigation of Separated Nozzle Flows. *AIAA J.* **1994**, *32*, 1836–1843. [CrossRef]